1. Introduction

Over the past years considerable research efforts have been devoted to the study of natural convection in rectangular and square cross section enclosures. The literature is vast on this subject, both when the enclosure is filled with a single fluid or filled with a fluid saturated porous medium. An excellent overview of such body of work can be found in [1-3]. The search for efficient thermal systems has led to different strategies, which include, among others, partitioned enclosures [4–6], enclosures with triangular cross-sections [7-8] or with trapezoidal cross-sections [9], fins attached to the active enclosure walls [10–16].

Buoyancy-driven convection in a sealed enclosure with differentially heated isothermal vertical walls is a prototype of many industrial applications such as ventilation of rooms, solar energy collection, dispersion of waste heat in reactor insulation and cooling of radioactive waste container. Enhancement of heat transfer by adding extended surfaces with good thermal conductivity on the heated surface for the purpose of cooling, as in electronic packages has received some consideration in recent years. Fu *et al.* [10] employed penalty finite-element method with a Newton-Raphson iteration algorithm to solve transient natural convection in an enclosure partitioned by an adiabatic baffle. The results indicated that the steady time and the strength of stream function strongly depend on the location of the baffle and the Rayleigh number. Natural convection in a differentially heated rectangular cavity with multiple conducting baffles on the cold wall was reported by Scozia *et al.* [11] for different values of Rayleigh number. As the inter-baffle ratio was varied from 0.25 to 20, the flow patterns evolved considerably and the average Nusselt number exhibited maximum and minimum values, whose locations depended on the value of Rayleigh number. Natural convection in the central micro-cavities of vertical, finned cavities of very high aspect ratios was numerically investigated by Frederick *et al.* [12]. Equally spaced baffles, located on both active walls, were considered. The dependence of micro-cavity circulation rates and heat transfer on Rayleigh number, dimensionless fin length, and micro-cavity aspect ratio is discussed. The average Nusselt number in a region comprising two consecutive micro-cavities was higher than the one observed when the baffles were attached to only one of the active walls. Yucel *et al.* [13] investigated numerically the natural convection in an enclosure with perfectly conducting horizontal end walls and finitely conducting baffles. Results were obtained using the Boussinesq model for density variation, showed good agreement with reported measurements of natural convection in a partitioned enclosure. Sezai *et al.* [14] investigated the effect of attaching poor conductor ribs on a vertical heated plate. The effects of rib height to span ratio and Rayleigh number are investigated experimentally and numerically for air as the working fluid. It was found that, adding ribs on the surface can reduce the rate of free convection heat transfer by as much as 75% compared with a bare plate. Rather, complex recirculation flow pattern was predicted in the space between the ribs at high Rayleigh numbers. The effects of baffle height, length and Rayleigh number on heat transfer performance was investigated numerically by Tasnim *et al.* [15]. It was found that adding baffle on the hot wall increase the heat transfer by as much as

21.4% compared with a bare wall for $Ra=10^4$. Silva *et al.* [16] investigated the effect of the aspect ratio and horizontal length of a high conductivity rectangular fin attached to the hot wall of a three-dimensional differentially heated cubic enclosure in laminar natural convection. The numerical results showed that for an enclosure assisted by a large volume fraction fin, the fin aspect ratio does not play an important role and the average heat flux transferred to the fluid increases monotonically with the fin horizontal length.

In the present study a detailed analysis was performed to check the effect of length and height of a conductive single and multiple baffle of finite thickness, which is attached to hot vertical wall, on heat transfer of a square enclosure. Rayleigh number in the range of 10^2-10^6 is considered for air as working fluid. Baffle length varies from 0.1 to 0.9. Dimensionless baffle position varies from 0.2 to 0.8 respectively, considering single baffle configuration. The numbers of attached baffles, which equally divided hot wall, are varied up to 4 baffles considering multi baffles configuration.

2. Problem formulation

The studied configuration, depicted in figure (1), is a square enclosure of length L. It is assumed that the third dimension of the enclosure is large enough so that the fluid flow and heat and mass transfer can be considered two-dimensional. The top and bottom walls are thermally insulated, whereas the left wall is maintained hot at high temperature (T_h) and right wall is maintained cold at low temperature (T_c). A horizontal baffle is attached to different positions on the hot active wall considering single baffle problem. In addition, equal divided baffles are attached to hot active wall considering multi-baffle problem. The enclosure vertical walls and baffles are made of conductive material. Both left hot wall and baffles are considered maintained at the same temperature. Where, W and H are represented the dimensionless length and the height of the baffle from the bottom insulated wall respectively. Rayleigh number, W, H and number of attached baffles are considered problem parameters.

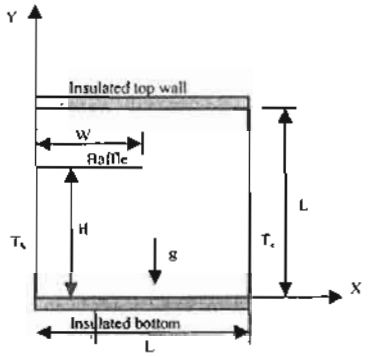

Fig. (1) Physical model and geometry.

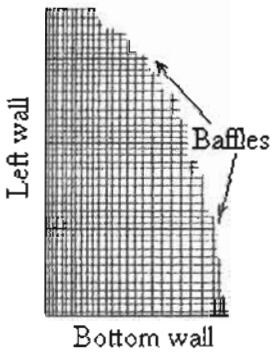

Fig. (2) Grid details.

3. Mathematical Modeling

The air properties were assumed to be constant and evaluated at a reference temperature, $T_o = (T_h + T_c)/2$, except for the density, which is treated with the Boussinesq approximation. To put the governing equations and their boundary and initial conditions in dimensionless form, one introduces the following dimensionless independent and dependent variables as [15,17];

$$X=\frac{x}{L}, Y=\frac{y}{L}, U=u\frac{L}{\alpha}, V=v\frac{L}{\alpha},$$

$$P=\frac{pL^2}{\rho\alpha^2}, \theta=\frac{(T-T_c)}{(T_h-T_c)} \quad (1)$$

Variables u, v, T and p are the velocity components in x, y directions, temperature and pressure respectively. Using the foregoing defined dimensionless variables and with the assumption of two-dimensional steady-state condition, the governing equations take the following form;

$$\frac{\partial U}{\partial X}+\frac{\partial V}{\partial Y}=0 \quad (2)$$

$$U.\frac{\partial U}{\partial X}+V\frac{\partial U}{\partial Y}= -\frac{\partial P}{\partial X}+\Pr\left(\frac{\partial^2 U}{\partial X^2}+\frac{\partial^2 U}{\partial Y^2}\right) \quad (3)$$

$$U.\frac{\partial V}{\partial X}+V\frac{\partial V}{\partial Y}= -\frac{\partial P}{\partial Y}+\Pr\left[\left(\frac{\partial^2 V}{\partial X^2}+\frac{\partial^2 V}{\partial Y^2}\right)+Ra\cdot\theta\right] \quad (4)$$

$$U\frac{\partial \theta}{\partial X}+V\frac{\partial \theta}{\partial Y}=\frac{\partial^2 \theta}{\partial X^2}+\frac{\partial^2 \theta}{\partial Y^2} \quad (5)$$

Where, Pr and Ra are the Prandtl and Rayleigh numbers, which are defined according to the following equations;

$$Pr=\frac{\nu}{\alpha} \;\&\; Ra=\frac{g.\beta.(T_h-T_c)}{\alpha.\nu} \quad (6)$$

The dimensionless forms of boundary conditions are;

at X = 0, for $0 \le Y \le 1$

U = V = 0 and $\theta = 1$

at X = 1, for $0 \le Y \le 1$

U = V = 0 and $\theta = 0$

at Y = 0, 1 for $0 \le X \le 1$

$$U = V = 0 \text{ and } \frac{\partial \theta}{\partial Y} = 0$$

at the baffle surface Y=H, $0 \le X \le W$

U = V = 0 and $\theta = 1$ (7)

From the engineering point of view, the most important characteristic of the flow is the rate of heat transfer across the enclosure; this is the local and average Nusselt number (Nu_L, Nu). Both, the local and average Nusselt number are calculated as;

$$Nu_l=\left(-\frac{\partial \theta}{\partial n}\right)_s \quad (8)$$

$$Nu=\frac{1}{s}\int_s Nu_l\, ds \quad (9)$$

Where, s is the surface of left hot wall and baffle(s).

4. Numerical Technique

The governing equations are discretized according to the central finite divided difference scheme. The first and second derivatives with respect to X and Y are approximated by centered finite difference. The partial differential forms of governing equations are transformed to sets of linear algebric equations. Solving these sets of equations, using Gauss-Siedle iterative procedure, the hydrodynamic and thermal flow fields can be obtained. Consequently, local and average Nusselt number can be derived with the aid of their definitions. A non-uniform grid of 150 × 150 was used, considering intense grid near the walls and baffles as shown in figure (2). Comparison of the Nusselt number values with those obtained at higher grid size give nearly identical results. Variations by less than 10^{-6} over all grid points were adopted as a convergence criterion. The code was checked using the results reported in the references [1], [15]. Tables 1 gives the values of average Nusselt number for the hot wall for Ra = 10^4, 10^5 and 10^6 for a square enclosure without attached baffles. These values are found to be in good agreement with references [1] AND [15].

Table 1: Code validation test with references [1 and 15].

Ra	10^4	10^5	10^6
Ostrach [1]	2.234	4.521	8.798
Tasnim [15]	2.244	4.5236	8.854
Present study	2.285	4.583	8.684

5. Results and discussions

5.1 Stream lines

Figures 3(a) to 3(d) show the stream lines for the case of Ra = 10^6 with a single baffle length of W = 0.6 for different baffle position of H = 0.2, 0.4, 0.6 and 0.8 respectively. The plots are arranged going from left to right with the ascending of H values. For all baffle positions a large clockwise rotating cell was observed. The fluid that is heated next to hot wall rises and replaces the fluid cooled next to cold wall that is falling, thus giving rise to a clockwise rotating vortex. Also it is clear that, a baffle attached to near the middle of the hot wall has the most remarkable effect on the fluid flow inside enclosure. A baffle placed at H $\leq$ 0.2, redirects the movement of the fluid and weakens the fluid motion within the area under the baffle whereas baffle at H $\geq$ 0.6 it weakens the fluid motion within the area above the baffle [15].

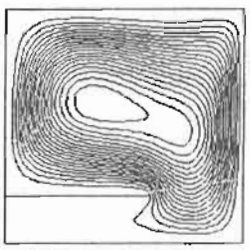

(a) H = 0.2, ψ_m = 0.018

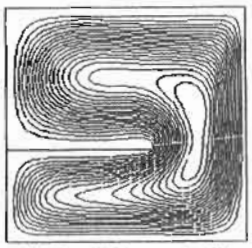

(b) H = 0.4, ψ_m = 0.031

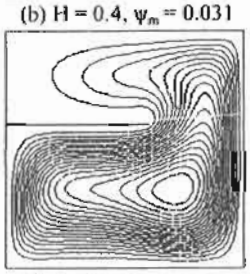

(c) H = 0.4, ψ_m = 0.026

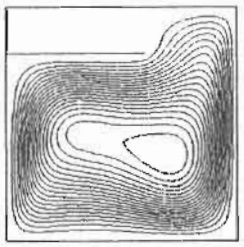

(d) H = 0.2, ψ_m = 0.021

Fig. (3) Stream lines with single baffle.

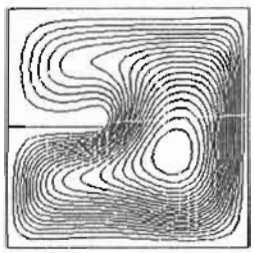

(a) 1 baffle, H=0.5, ψ_m = 0.038

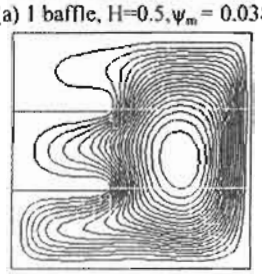

(b) 2 baffles, ψ_m = 0.021

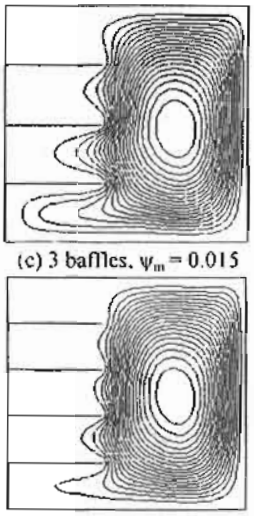

(c) 3 baffles, $\psi_m = 0.015$

(d) 4 baffles, $\psi_m = 0.009$

Fig. (4) Stream lines with single baffle and multi-baffles

Figures 4(a) to 4(d) show the stream lines for the case of Ra = 10^6 with baffle length of W = 0.4 for different numbers of attached baffles. The baffles which equally divided the hot wall have the values of 1 (single), 2, 3 and 4. For single baffle, the presence and character of clockwise rotating vortex is unaltered with a shorter baffle as shown in figure 4 (a). Considering 2 and 3 baffles configuration, the air flows smoothly, contouring the cavity formed by the baffles, especially lower ones, with no recirculation in between as shown in figure 4 (b) and 4 (c). Increasing the number of baffles attached to hot wall leads to suppress the flow, and vortex flow zone is formed directly at the baffles tips as shown in figure 4 (d).

5.2 Temperature distribution

Figures 5 and 6 show the temperature distribution, θ $(T-T_c/T_h-T_c)$, as a function of the distance, X (x/L), from the hot wall to the cold wall of the enclosure. The dimensionless temperature profile for a given vertical position, Y (y/L) are plotted for Y= 0.2, 0.4, 0.6 and 0.8.

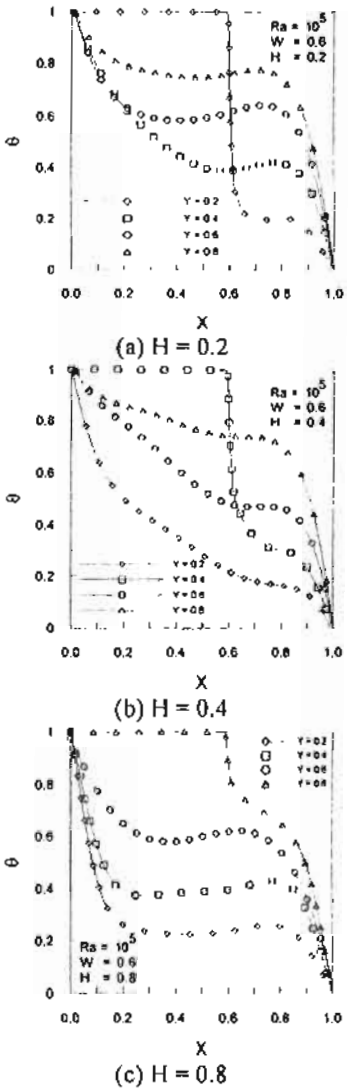

Fig. (5) Temperature distribution for single baffle at different vertical positions.

For single baffle configuration with baffle length W = 0.6 and baffle position of H = 0.2, 0.4 and 0.8 at Ra = 10^5, the temperature profiles disclose a steep drop of temperature along the hot and cold walls with a slightly linear temperature increase in the central core as shown in figures 5(a) to s(c). This result indicates that in addition to the heat transported by natural convection along the surface of hot, cold and baffle walls, there is heat conduction through the central core of the layer. The increase of temperature in the core is

attributed to the presence of hot baffle. As the values of H increased ($H \geq 0.5$), the fluid motion in the area above the baffle is weaken and thus decrease heat transfer capabilities is expected. The values of temperature under the baffle are decreased with the increase of baffle height H. this implies better heat transfer on the bottom of the baffle than on the top surface when $H \geq 0.5$ and vice versa.

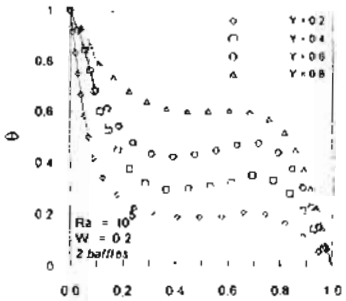

(a) 2 baffles

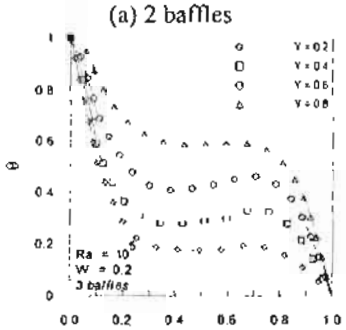

(b) 3 baffles

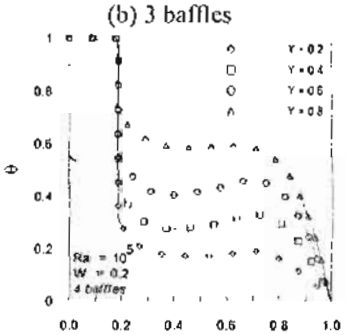

(c) 4 baffles

Fig. (6) Temperature distribution for multi baffles configuration.

Considering multi baffles configuration, figure 6(a) to 6(c) show temperature distribution for baffle length $W = 0.2$ and $Ra = 10^5$ with different number of baffles attached to the hot surface. It is observed that, a steep drop of temperature in the region immediately adjacent to both hot and cold walls and an almost horizontal temperature distribution is found in the central core of the enclosure.

5.3 Local Nusselt number on the left hot wall

It is necessary to observe the variations of the local Nusselt number on the hot wall in order to evaluate the effects of baffles attached to the hot wall. Figure (7) shows distribution of local Nusselt number (Nu_L) along the left wall for $Ra = 10^5$ and $W = 0.4$, the single baffle configuration at different positions and the multi baffles configuration.

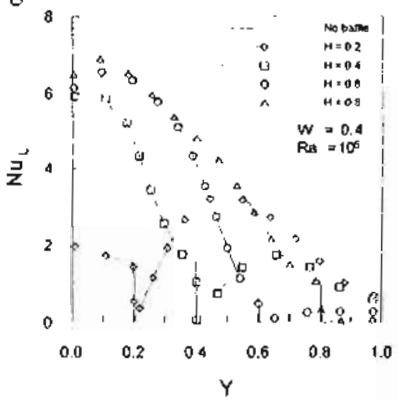

(a) Single baffle at different positions

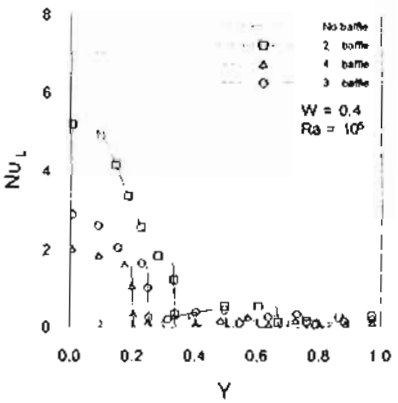

(b) Multi baffles

Fig. (7) Local Nusselt number distribution along left hot wall.

In general from figure (7), one can observe that placing baffles on the hot wall always reduce local Nusselt number on this wall compare with bare wall. This is because the baffle blocks the flow near it, thus giving rice to different flow patterns on the top and bottom of the baffle depending on length, position and number of the used baffle [9, 15]. For single baffle configuration shown in figure 7(a), as the value of H increased the boundary layer on the hot wall is altered (referring to figure 3) and significant separated region is observed. While the development of the boundary layer on the left wall under the baffle is unaltered. The variation of local Nusselt number on these two parts of the hot wall are directed linked to the two distinct flow patterns causing significant heat transfer reduction below the baffle. At lower values of H, Nusselt number increases at the top region of the baffle compared with the bottom region of the baffle. These results are achieved considering multi baffle configuration as shown in figure 7(b). For any number of baffles attached to the hot wall, higher values of local Nusselt number are obtained in the region to the bottom of first baffle and deteriorated elsewhere [14]. Even though a baffle attached to hot wall always reduces the heat transfer on this wall, this does not mean that the heat flux through the enclosure will be reduced because the conductive baffle also transfers heat into the enclosure.

5.4 Average Nusselt number

To evaluate the effect of attaching conducting baffles on the average heat transfer, the average Nusselt number (Nu) is plotted as a function Rayleigh number for single and multi baffles configurations as shown in figures 8 and 9. For single baffle configuration, figures 8(a) to 8(c) are plotted for different values of baffle length W with baffle position H =0.2, 0.4 and 0.6 respectively. It observed that, the average Nusselt number is increased with the increase of the Rayleigh number or the baffle length W. The data appear to be nearly independent of baffle position. At values of Ra up to 10^4, the values of the average Nusselt number are, almost, the same since the clockwise rotating vortex is unaltered. As seen as, the average Nusselt number increases with the increase of Ra.

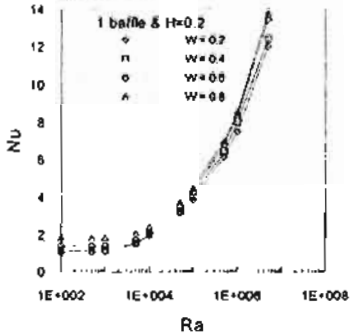

(a) H = 0.2

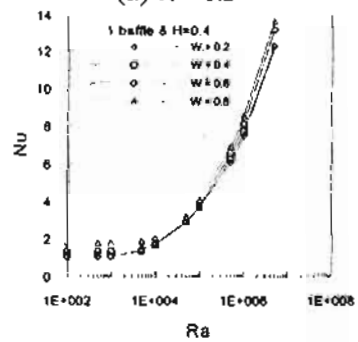

(b) H = 0.4

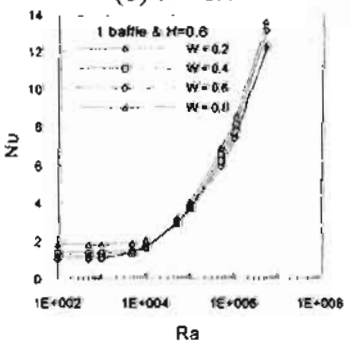

(c) H = 0.6

Fig.(8) Average Nusselt number distribution as a function of Rayleigh number, single baffle configuration.

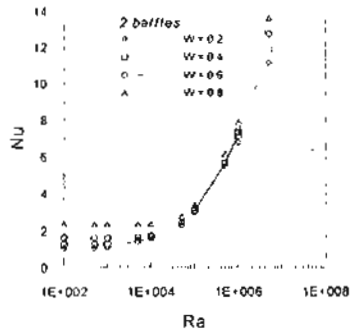

(a) 2 baffles

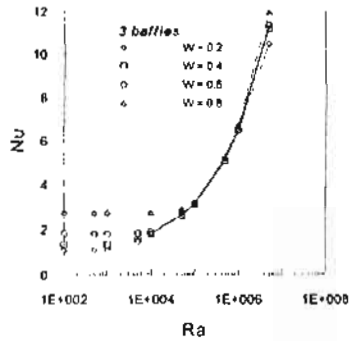

(b) 3 baffles

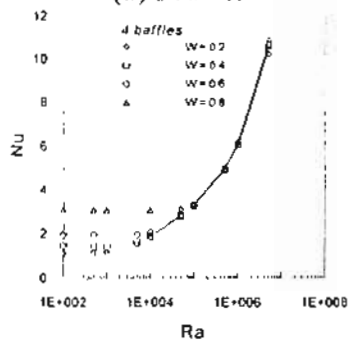

(c) 4 baffles

Fig.(9) Average Nusselt number distribution as a function of Rayleigh number, multi baffles configuration.

These results are the same for multi baffle configuration as shown in figures 9(a) to 9(c). For $Ra \geq 10^5$, it is clear that, as the numbers of attached baffles increase the Nusselt number is decreased. This is attributed to the flow blockage which formed by introducing baffles. For $Ra \leq 10^5$ and long baffle length, increasing the number of baffles increases the average Nusselt number. Since the long baffles acts as bridge between hot and cold wall, in addition, they partially divided the enclosure to several adjacent cavities.

Finally, the average Nusselt number is plotted as a function of baffle length W as shown in figures 10(a) to 10(c) for three different baffle positions and for different values of Rayleigh number considering single baffle configuration. It is clear that, the average Nusselt number increases with the increase of W. The longest baffle gives the best results and it is independent of baffle position as early explained. For longest baffle and $Ra = 10^6$ the increase in the rate of heat transfer is 11.52 % higher that in enclosure without baffle.

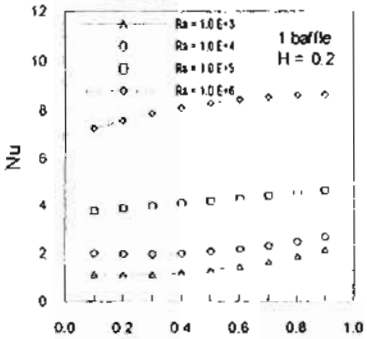

(a) H = 0.2

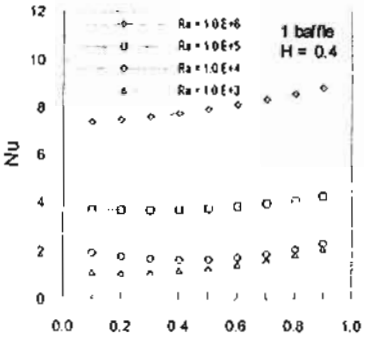

(b) H = 0.4

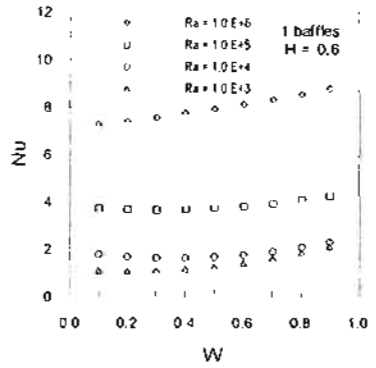

(c) H = 0.6

Fig. (10) Average Nusselt number distribution as a function of baffle length, single baffle configuration.

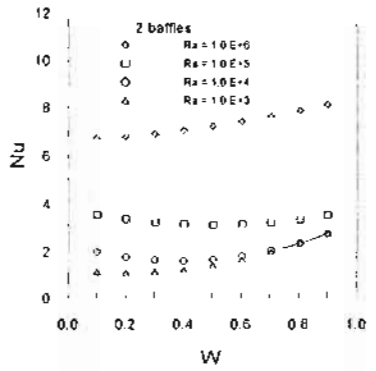

(a) 2 baffles

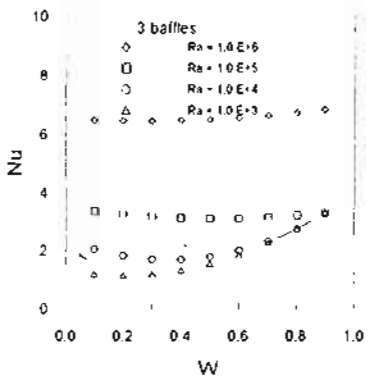

(b) 3 baffles

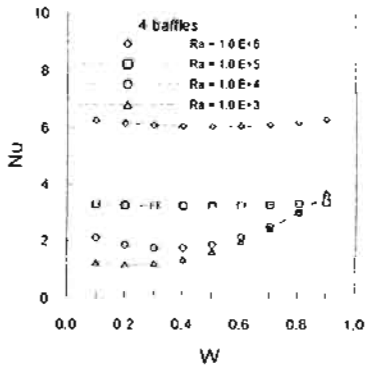

(c) 4 baffles

Fig. (11) Average Nusselt number distribution as a function of baffle length, multi baffles configuration.

Considering multi baffles, figures 11(a) to 11(c) show the average Nusselt number as a function of W under the above mentioned conditions. At Ra = 10^3 and baffle length $W \leq 0.4$, Nu is the same for all baffle positions H. But for $W \geq 0.4$, the average Nusselt number increases sharply with the increase of baffle length. Increasing numbers of baffles mounted on hot wall and the values of Rayleigh number, the average Nusselt number becomes independent of baffle length.

6. Conclusions

The flow and heat transfer in a square enclosure with thin horizontal conductive baffles on the hot wall are theoretically investigated. Rayleigh number, baffle length, baffle position and the numbers of attached baffles are proposed as problem parameters. Generally, the attached baffle modifies the clockwise rotating vortex that is established because of differentially heated walls. The blockage effect of the baffle depends on baffle length. Depending on Rayleigh number, length of baffle, baffle position and number of baffles, a number of recirculation regions can be formed above and under the baffle. Placing baffles on the hot wall

always reduce local Nusselt number on this wall compare with bare wall. On the other hand, the extra heating effect which offered by the baffle is promoted as the Rayleigh number increases. It observed that, the average Nusselt number is increased with increasing baffle length while it is independent of baffle position. For longest baffle and Ra = 10^6 the increase of heat transfer is 11.52 % higher than that increase in enclosure without baffle considering single baffle configuration.

References

[1] S. Ostrach, Natural convection in enclosures, ASME J. Heat Transfer 110 (1988) 1175–1189.

[2] A. Bejan, Convection Heat Transfer, 2nd edition, Wiley, New York, Chapter 5, (1995).

[3] J. N. Arnold, D. K. Edwards and I. Catton, Effect of tilt and horizontal aspect ratio on natural convection in a rectangular honeycomb, ASME J. Heat Transfer 99 (1977) 120–122.

[4] R.L. Frederick, A. Valencia, Heat transfer in a square cavity with a conducting partition on its hot wall, Int. Comm. Heat Mass Transfer 16 (1989) 347–354.

[5] E. Zimmerman, S. Acharya, Free convection heat transfer in a partially divided vertical enclosure with conducting end walls, Int. J. Heat Mass Transfer 30 (1987) 319–331.

[6] T. Nishimura, Natural convection in horizontal enclosures with multiple partitions, Int. J. Heat Mass Transfer 32 (9) (1989) 1641–1647.

[7] D. Poulikakos, A. Bejan, Natural convection experiments in a triangular enclosure, ASME J. Heat Transfer 105 (1983) 652–655.

[8] H. Salmun, Convection patterns in a triangular domain, Int. J. Heat Mass Transfer 38 (2) (1995) 351–362.

[9] F. Moukalled, S. Acharya, Natural convection in trapezoidal cavities with baffles mounted to their upper inclined surfaces, Num. Heat Transfer A 37 (2000) 545–565.

[10] W.S. Fu, J.C. Perng and W.J. Shieh, Transient laminar natural convection in an enclosure partitioned by an adiabatic baffle, Numerical Heat Transfer 16 (A), 535-350, (1989).

[11] R. Scozia, R.L. Frederick, Natural convection in slender cavities with multiple fins attached to an active wall, Num. Heat Transfer: Part A 20 (1991) 127–158.

[12] R.L. Frederick, A. Valencia, Natural convection in central micro-cavities of vertical, finned enclosures of very high aspect ratio, Int. J. Heat Fluid Flow 16 (1995) 114– 124.

[13] N. Yucel, H. Turkoglu, Numerical analysis of laminar natural convection in enclosures with fins attached to an active wall, J. Heat Mass Transfer 33 (1998) 307–314.

[14] I. Sezai, A.A. Mohamad, Suppressing free convection from a flat plate with poor conductor ribs, Int. J. Heat and Mass Transfer 42 (1999) 2041-2051.

[15] S.Y. Tasnim, M. R. Collins, Numerical analysis of heat transfer in a square cavity with a baffle on the hot wall, Int. Comm. Heat Mass Transfer 31 (2004) 639–650.

[16] A.K. da Silva, L. Gosselin, On the thermal performance of an internally finned three-dimensional cubic enclosure in natural convection, Int. J. Thermal Sciences 44 (2005) 540–546.

[17] P. Oosthuizen and D. Naylor, Introduction to Convection Heat Transfer Analysis, McGraw-Hill, Chapter 8, (1999).